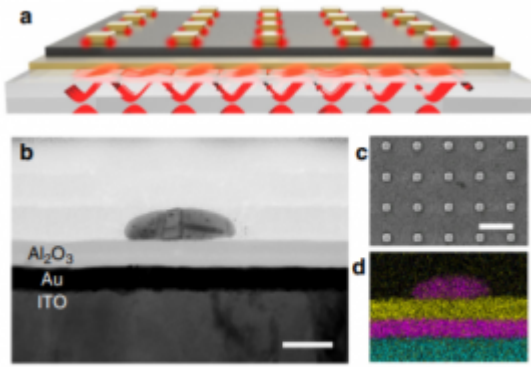


Manipulation of the dephasing time by strong coupling between localized and propagating surface plasmon modes

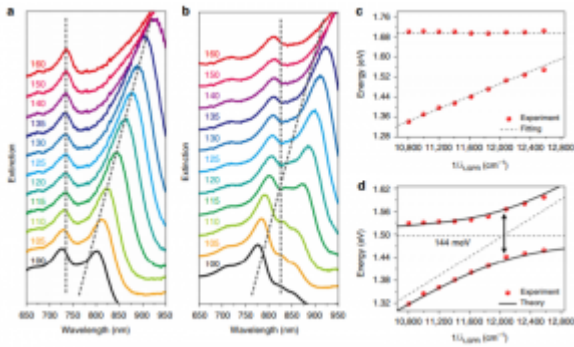
Strong coupling between two resonance modes leads to the formation of new hybrid modes exhibiting disparate characteristics owing to the reversible exchange of information between different uncoupled modes. Here, we realize the strong coupling between the localized surface plasmon resonance and surface plasmon polariton Bloch wave using multilayer nanostructures. An anticrossing behavior with a splitting energy of 144 meV can be observed from the far-field spectra. More importantly, we investigate the near-field properties in both the frequency and time domains using photoemission electron microscopy. In the frequency domain, the near-field spectra visually demonstrate normal-mode splitting and display the extent of coupling. Importantly, the variation of the dephasing time of the hybrid modes against the detuning is observed directly in the time domain. These findings signify the evolution of the dissipation and the exchange of information in plasmonic strong coupling systems and pave the way to manipulate the dephasing time of plasmon modes, which can benefit many applications of plasmonics.



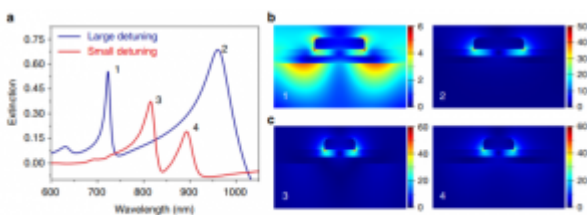
Structural characterization. The structure designed to realize the strong coupling is shown in Fig. 1. A 20-nm-thick gold film is deposited on an indium-tin-oxide (ITO)-coated glass substrate to support the SPP-Bloch wave. The ITO layer has a thickness of 150 nm, which makes the entire substrate surface suitably conductive for PEEM measurements. Then, a 25-nm-thick Al₂O₃ spacer is deposited using the atomic layer deposition technique.

The gold square nanoblock arrays are fabricated on the Al₂O₃ spacer via electron-beam lithography (EBL), followed by metal sputtering and lift-off, to support the LSPR modes. The sectional view (Fig. 1b) and top view (Fig. 1c) of the sample are acquired by a scanning transmission electron microscope (STEM) and a scanning electron microscope (SEM), respectively. In addition, energy-dispersive X-ray spectroscopy (EDS) is used to mark

different elements with a distinct color in the sectional view (Fig. 1d). The nanoblocks of different sizes (side lengths) are designed (100–160 nm) to tune the LSPR energy. Beyond that, the nanoblock array can provide the additional wave vector for the excitation light (k_0) to excite the SPP supported on the thin metal by compensating the momentum mismatch between the excitation light and the SPP modes.



Experimental far-field spectral property. The measured extinction spectra of samples with different nanoblock sizes and fixed periods (400 or 500 nm) are presented in Fig. 2a, b, respectively. For the period of 400 nm, the left peak is almost entirely unshifted, and the right peak undergoes a redshift as the nanoblock size increases. The left and right peaks can be assigned to the SPP Bloch wave and LSPR mode, respectively. Moreover, in this case the two modes cannot couple well with each other, as is clearly shown by the dispersion curves of the two modes (Fig. 2c), where the SPP modes are kept unchanged while the nanoblock sizes change. Similarly, the dissipation of the LSPR mode ($\gamma_{\text{LSPR}} = 98$ meV) and the SPP-Bloch waves ($\gamma_{\text{SPP}} = 38$ meV) can be calculated from the experimental line widths with a period of 400 nm and a nanoblock size of 135 nm. For the period of 500 nm, the dispersion curves (Fig. 2d) extracted from the extinction spectra show an anticrossing behavior and can be fitted by the coupled oscillator model^{9,22,26} (details are shown in the Supplementary Note 1). The splitting energy is calculated as 144 meV at $E_{\text{LSPR}} = E_{\text{SPP}}$. Then, we can determine that the interaction potential (V) is 78 meV.



Simulation results. To further understand these modes, we

use the finite-difference time domain (FDTD) method to simulate the mode distribution. With the large nanoblock size (150 nm) and the small period (400 nm), two peaks appear on the extinction spectrum (blue line in Fig. 3a). Peak 1 has a narrow line width, and the electric field is confined mainly on the lower surface of the Au film. Peak 2 has a broad line width, and the electric field is located mainly at the interface between the nanoblocks and Al₂O₃, with much greater field enhancement, as shown in Fig. Therefore, we recognize that peaks 1 and 2 represent the SPPBloch wave and LSPR mode, respectively, and that the detuning between the LSPR mode and SPP-Bloch wave is large (~396 meV) in this case. The energy exchange gives rise to a higher near-field enhancement than the single SPP-Bloch wave and a longer oscillation time than the single LSPR mode, which demonstrates that the coupling between the LSPR mode and SPP-Bloch wave modifies the field distribution resulting from the normal-mode splitting with the small detuning. Notably, the near-field enhancement of the two coupled modes (peaks 3 and 4) is both present and, in fact, slightly higher than that of the LSPR mode only (peak 2), which is shown by Fig.

For more information: DOI: 10.1038/s41467-018-07356-x